Bulletin of the Geological Survey of Japan, vol. 75 (2), p. 61–72, 2024

Report

Zircon U–Pb age constraints on the history of Carboniferous volcanism in the South Kitakami Belt, Northeast Japan

KAWAMURA Toshio[1, 2, *] and UCHINO Takayuki[2]

KAWAMURA Toshio and UCHINO Takayuki (2024) Zircon U–Pb age constraints on the history of Carboniferous volcanism in the South Kitakami Belt, Northeast Japan. *Bulletin of the Geological Survey of Japan*, vol. 75 (2), p. 61–72, 5 figs and 3 tables.

Abstract: Carboniferous strata of the South Kitakami Belt in Northeast Japan contain large volumes of volcaniclastic rocks that indicate intense volcanism. We conducted zircon U–Pb dating on samples collected from two stratigraphic horizons: coarse felsic tuff from the middle part of the lower Carboniferous Shittakazawa Formation, and sandy tuff from the middle part of the upper Carboniferous Kidoguchi Formation. The samples yielded weighted mean ages of 339.5 ± 2.6 Ma (middle Visean) and 313.6 ± 2.3 Ma (early Moscovian), respectively. The former age is more tightly constrained and slightly younger than the late Tournaisian age previously determined using fossil biostratigraphy and lithostratigraphic correlations. The latter age indicates that volcanism was ongoing throughout the late Carboniferous. Taking into account the occurrence of late Carboniferous granitic rocks and earliest Permian andesitic tuff in the South Kitakami Belt, our results suggest that igneous activity lasted from the Carboniferous to early Permian.

Keywords: zircon U–Pb dating, Carboniferous, Visean, Moscovian, volcanism, South Kitakami Belt, Kitakami Massif, Setamai, Oide, Iwate Prefecture

1. Introduction

The South Kitakami Belt (SKB) in Northeast Japan contains thick sequences of coherent Carboniferous strata dominated by volcanic rocks and limestone (Kawamura and Kawamura, 1989a), in contrast to exotic bodies of seamount rocks in late Paleozoic and Mesozoic accretionary complexes such as the Akiyoshi, Mino–Tanba, and Chichibu belts. The Carboniferous sequences represent intense volcanism in and around an island arc, and subsequent less-intense but continuous minor to moderate volcanism near a carbonate shelf (Kawamura and Kawamura, 1989b). These sequences are unconformably overlain by Permian clastic sedimentary rocks that were deposited in a shelf environment (Kawamura *et al.*, 1990). This change from Carboniferous volcanism to Permian minor volcanism or quiescence represents a key tectonic transition of the SKB from an active to a passive margin (Ehiro *et al.*, 2016).

The Carboniferous sequence in the SKB comprises mainly volcaniclastic and terrigenous clastic rocks in the lower section and carbonate rocks interlayered with volcaniclastic rocks in the upper section. Volcaniclastic rocks of the lower section have both basaltic and rhyolitic–dacitic compositions but lack typical andesite (i.e., bimodal volcanism), suggesting they formed in an extensional region such as an intra-arc or back-arc setting (Kawamura and Kawamura, 1989b). In contrast, volcaniclastic rocks of the upper section consist mainly of felsic or intermediate tuff. The contrasting lithologies of the two sections imply a minor change in volcanism and tectonic setting after the early Carboniferous. However, the ages and geochemical signatures of the rocks of the two sections have yet to be fully investigated.

The ages of these Carboniferous strata have been determined by fossil fauna and litho- and biostratigraphic correlations (e.g., Minato *et al.*, 1979). Paleontological evidence indicates that the lower section is the upper Tournaisian to middle–upper Visean (Kawamura, 1983). The limestone in the lower part of the upper section has traditionally been assigned to the upper Visean based on the characteristic coral fauna (UVCF; Niikawa, 1983), and the other parts of the upper section are correlated to the Namurian to lower Westphalian (i.e., Serpukhovian to Moscovian; Minato *et al.*, 1979). These ages suggest that Carboniferous volcanism in the SKB continued for much of the period but was more intense during the early Carboniferous. However, reliable radiometric ages for the

[1] Miyagi University of Education, Sendai 980-0845, Japan
[2] AIST, Geological Survey of Japan, Research Institute of Geology and Geoinformation
[*] Corresponding author: KAWAMURA T., Email: t-kawa@staff.miyakyo-u.ac.jp

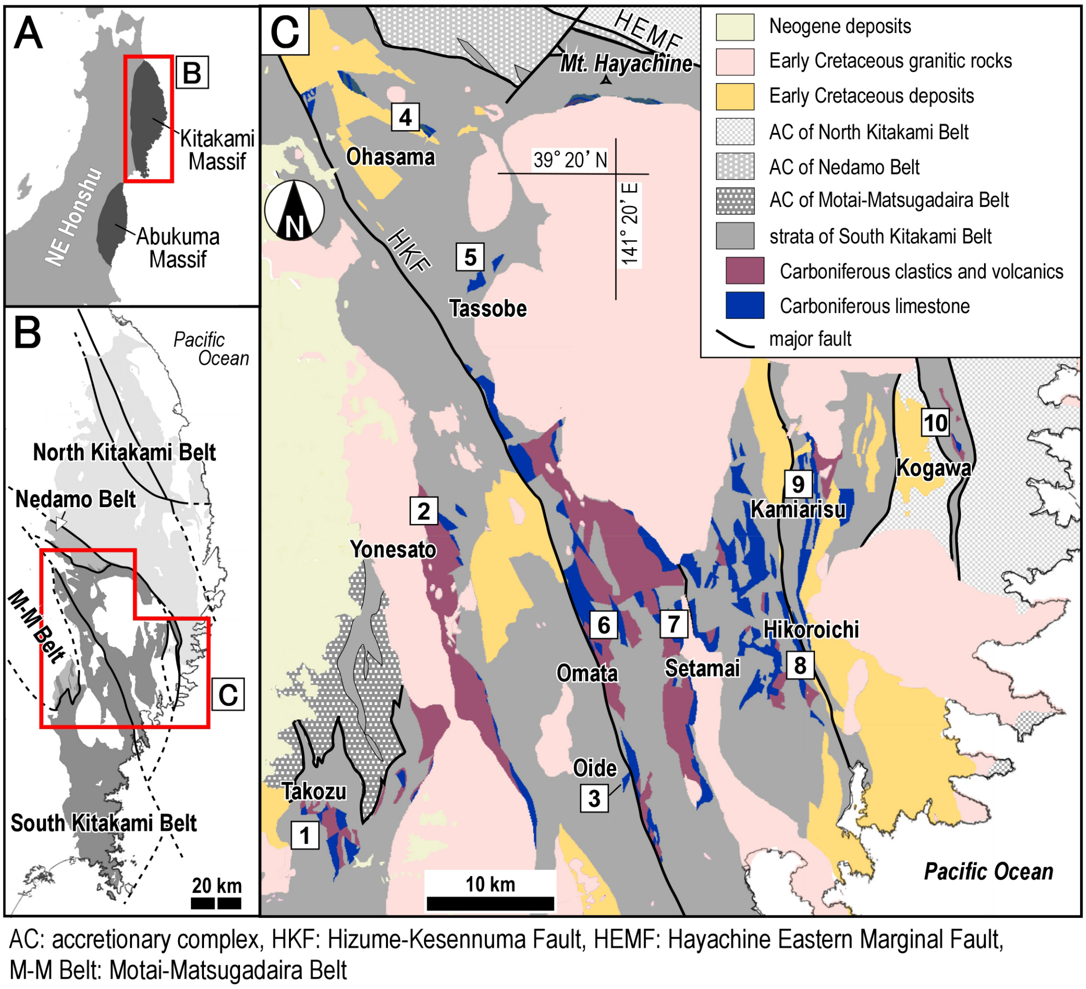

Fig. 1 (A) Index map of Tohoku district showing the Kitakami and Abukuma massifs. (B) Geologic belt in the Kitakami Massif. (C) Distributions of the Carboniferous sedimentary rocks in the South Kitakami Belt in the southern Kitakami Massif. Numbers are main areas where each Carboniferous stratigraphy is established. Distributions of the Carboniferous System is modified from the Seamless Digital Geological Map of Japan (1:200,000) V2 of the Geological Survey of Japan, AIST (2022). Quaternary covers are excluded.

clastic or volcanic rocks are limited to detrital zircon U–Pb ages for sandstones in the lower section (Okawa *et al.*, 2013; Pastor-Galán *et al.*, 2021). Accordingly, the detailed history of Carboniferous orogenic activity in the SKB remains poorly understood.

In this study, we conducted zircon U–Pb dating on two samples of felsic volcaniclastic rocks collected from the lower and upper sections. The dating results are used to cross-check fossil-based ages and constrain the history of Carboniferous volcanism in the SKB.

2. Geological outline

Carboniferous strata of the SKB are distributed mainly in the southern Kitakami Massif (Fig. 1) and at the eastern margin of the Abukuma Massif. The distribution of these strata is discontinuous due to the presence of unconformably overlying Permian and Mesozoic sedimentary rocks, the effects of faults and folds, and Cretaceous granitoid intrusions (Fig. 1C). The lithology and age differ among the 10 identified areas of exposures of these sedimentary rocks (Fig. 1C), meaning that the stratigraphy is established separately for each area (Fig. 2). Below, we outline the characteristics of the Carboniferous strata in these areas (Figs. 1C and 2), with a particular focus on stratigraphy and ages.

Lithostratigraphic correlations among the 10 areas allow the entire Carboniferous stratigraphic profile of the SKB to be divided into two sections: a lower clastic-dominated section (i.e., the Karaumedate, Yonesato, lower–middle Karosawa, Shittakazawa–Arisu–Odaira, Hikoroichi, and lower Kogawa formations in Fig. 2) and an upper carbonate-dominated section (i.e., the Takezawa, Shiba, Kidoguchi, Funakubo, Okawame, upper Karosawa–Senbakaya, Onimaru–Nagaiwa, Takasuzuyama, and upper Kogawa formations in Fig. 2) (Kawamura and Kawamura, 1989a). The lower section is

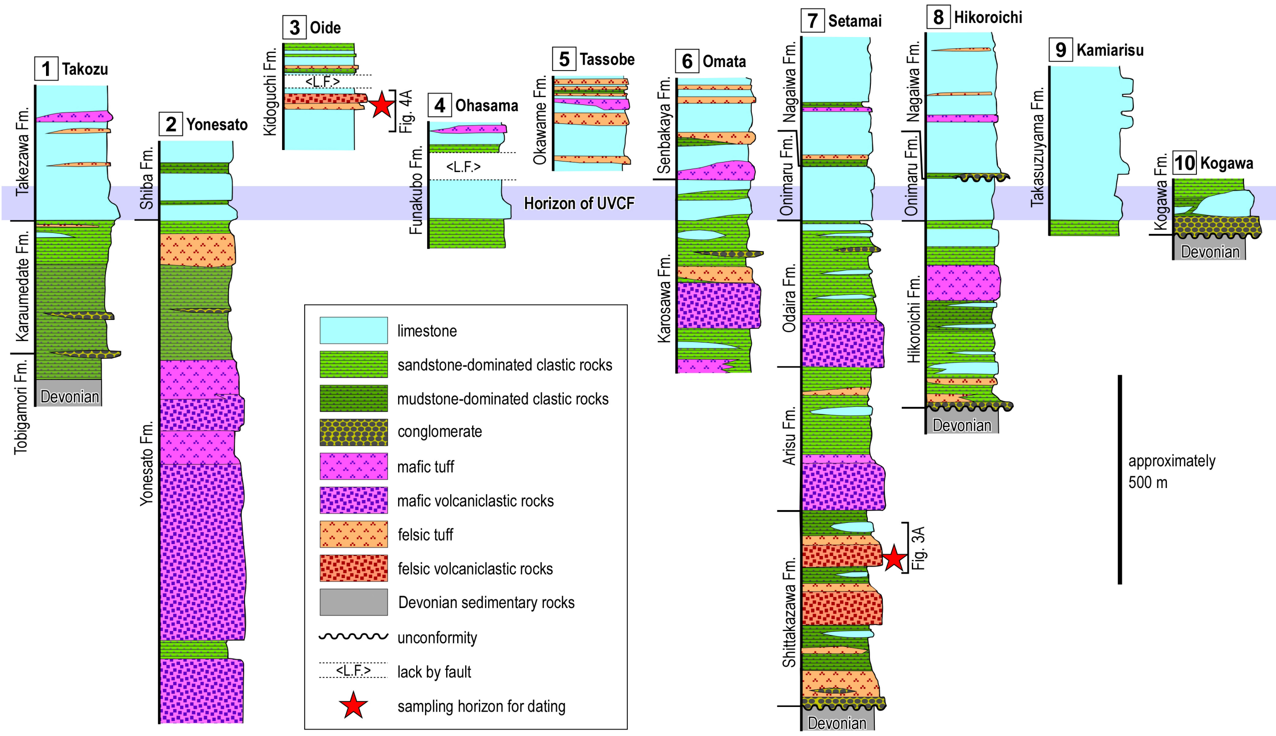

Fig. 2 Correlation of the generalized columnar sections for the Carboniferous stratigraphy in the main areas shown in Fig. 1C. Each column is arranged at the horizon of occurrences of the upper Visean coral fauna (UVCF). Fm.: Formation. Red star roughly shows the sampling horizon for dating in this study. The columns are modified from Kawamura and Kawamura (1989a).

composed of sandy clastic rocks and thick volcaniclastic rocks accompanied by lenticular limestone and conglomerate. The lowermost part of the section unconformably overlies Middle Devonian strata at the base in eastern areas (areas 7, 8, and 10 in Fig. 2) and conformably overlies Upper Devonian strata in the west (area 1 in Fig. 2). The depositional facies and thickness of the clastic rocks vary among the areas, suggesting deposition in heterogeneous sedimentary basins in and around a volcanic arc (Kawamura and Kawamura, 1989b). In contrast, the upper section, which conformably overlies strata of the lower section, is composed of carbonate rocks in all 10 areas. Abundant volcaniclastic rocks are intercalated with the carbonates of the upper section, especially in western–central areas (areas 2, 6, and 7 in Fig. 2). The main carbonate rocks are stratified shallow-marine limestone with localized limestone breccia, suggesting deposition in a carbonate-platform environment and subordinately in a marginal-slope environment (Kawamura and Kawamura, 1989b).

Volcaniclastic rocks of the lower section contain both basaltic and rhyolitic–dacitic resedimented pyroclastic rocks. These rocks are geochemically bimodal, without intermediate silica contents (Kawamura and Kawamura, 1989b; Kawamura, 1997). The chemical compositions of the basaltic rocks plot in the fields of island-arc tholeiite or calk-alkaline basalt (Kawamura, 1997). The early Carboniferous volcanism occurred in back-arc to intra-arc settings under crustal extension (Kawamura and Kawamura, 1989b). In contrast, volcaniclastic rocks of the upper section are mainly felsic or intermediate, although their geochemical signatures have yet to be defined in detail (Kawamura and Kawamura, 1989a). Their compositions suggest continuous volcanism in or around the area of carbonate deposition during the late Carboniferous.

The ages of the Carboniferous strata of the SKB have been determined using biostratigraphic correlations. The brachiopod fauna of the lower section is consistent with the late Tournaisian age for the lower part of the section and the early–middle Visean age for the upper part (Tazawa and Kurita, 2019; Tazawa, 2020). Similar age determinations have been obtained using coral and miospore fossils (Kawamura, 1983; Yang and Tazawa, 2000). A distinctive coral fauna in the lowermost limestone strata of the upper section has traditionally been regarded as being of the late Visean age (Fig. 2). The fusulinid and conodont biostratigraphy of the middle–upper strata of the upper section (Kobayashi, 1973; Minato *et al.* eds., 1979) indicates the Namurian to early Westphalian ages (i.e., Serpukhovian to Moscovian).

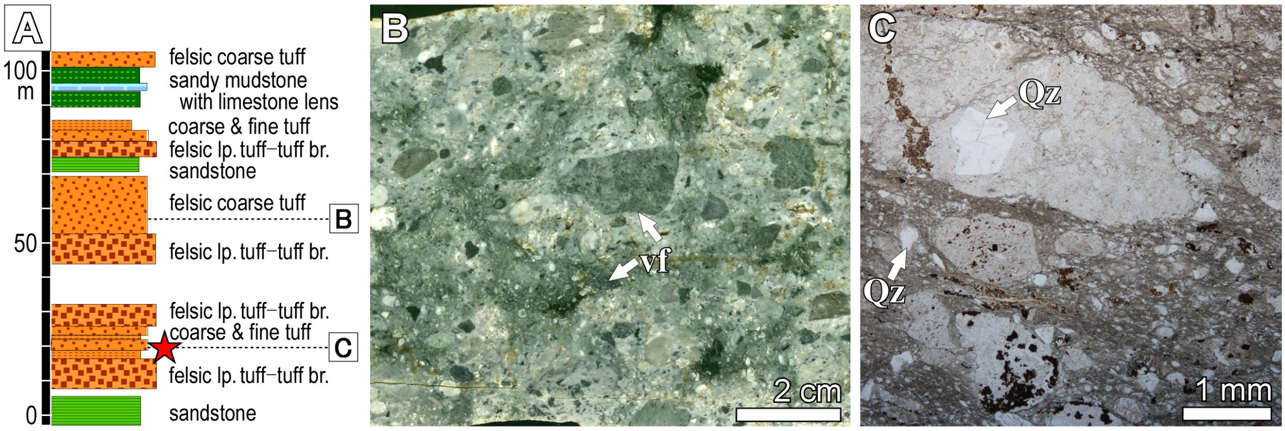

Fig. 3 (A) Columnar section around the horizon of the dating sample (22040401-1) in the lower Carboniferous Shittakazawa Formation. Northwest of Kashiwari, Setamai area, Sumita Town. The sampling horizon is shown as a red star. lp.: lapilli, br.: breccia. (B) Polished surface photo-image of the felsic coarse tuff in the lower part of a sequence suggesting pyroclastic density current deposits. Lithology shows inhomogeneous nature as commonly containing abundant fragments of felsic volcanic or volcaniclastic rocks. Northern creek of Kashiwari [39.16354N, 141.51363E], Setamai area, Sumita Town. (C) Thin-section photo-image of the dating specimen, plane-polarized light. Its lithology shows coarse tuff containing fragments of felsic volcanic rocks. Quartz fragments are present both in the glassy tuff matrix and the rock fragments. River cliff of the Omata River [39.16147N, 141.50637E], east of Komata, Setamai area, Sumita Town.
Qz: quartz, vf: volcanic rock fragment.

3. Samples for dating

Lower Carboniferous Shittakazawa Formation

The Shittakazawa Formation represents the lowermost part of the thick Carboniferous sedimentary rocks in the Setamai area (area 7 in Fig. 2) (Kawamura and Kawamura, 1989a). The formation consists of felsic volcaniclastic rocks, mudstone, and sandstone, with minor limestone lenses. A basal conglomerate and felsic tuff unconformably overlie Devonian strata, and the uppermost sandstone underlies basaltic volcaniclastic rocks of the Arisu Formation. The felsic volcaniclastic rocks, which comprise massive lapilli tuff, tuff breccia, and coarse tuff, fine upward to laminated fine vitric tuff and also intercalate fossil-bearing sandstone and mudstone, suggesting they represent subaqueous pyroclastic density current deposits on shallow-marine substrates (Kawamura, 1985; Kawamura, 1997).

Sample 22040401-1 was obtained from the middle Shittakazawa Formation, at a cliff adjacent to the Omata River (39.16147°N, 141.50637°E), east of Komata in the Setamai area, Sumita Town. The sample is greenish-gray coarse felsic tuff. In areas near the sampling location, this tuff is interbedded with fine tuff layers and overlies thick beds of lapilli tuff to tuff breccia (Fig. 3A). Similar bedding styles have been recognized in thick volcaniclastic rock sequences of the formation (Kawamura, 1997). The sample contains abundant fragments of dacite to rhyolite or volcaniclastic rocks, clasts of entirely chloritized flat pumice, and a matrix of fine glassy tuff with quartz and plagioclase grains (Fig. 3B and C). Quartz grains are also observed within rock fragments and commonly show corroded forms. Fine zircon grains are present within volcanic rock fragments or along dark seams in the tuff matrix.

Upper Carboniferous Kidoguchi Formation

The Carboniferous Kidoguchi Formation occurs in the Oide area (area 3 in Figs. 1C and 2) (Ehiro and Mori, 1993). The lower to middle parts of the formation are composed of limestone and volcaniclastic rocks. The upper part consists of limestone, tuff, and sandstone, unconformably overlain by the lower Permian sedimentary rocks. These units are equivalent to the Carboniferous sedimentary rocks at Tassobe (area 5 in Figs. 1C and 2) and Omata (area 6 in Figs. 1C and 2), which were probably connected to each other prior to lateral offset along a major sinistral fault (e.g., the Hizume Kesennuma Fault in Fig. 1) during the Early Cretaceous (Ehiro and Mori, 1993). Volcaniclastic rocks are generally predominant in the middle to upper Carboniferous sedimentary rocks in the western-central to northern-central areas of the SKB (3–6 in Fig. 1C).

Sample 22040115 was obtained from the lower Kidoguchi Formation at an outcrop on a forest trail in eastern Shizu (39.05935°N, 141.51294°E), Oide area, Yahagi Town, Rikuzentakata City. The sample is reddish-purple sandy tuff. At the outcrop, the tuff has a total thickness of 15 m, contains interbeds of greenish tuff, overlies gray limestone, and underlies felsic coarse tuff (Fig. 4A and B) of the middle part of the formation. The tuff consists of fragments of felsic volcanic or volcaniclastic rocks, plagioclase, and quartz in an inhomogeneous matrix of fine glassy silt (Fig. 4C). Volcanic rock fragments also contain quartz and plagioclase as phenocrysts. Concentrations of black hematite are commonly observed as grains, spots,

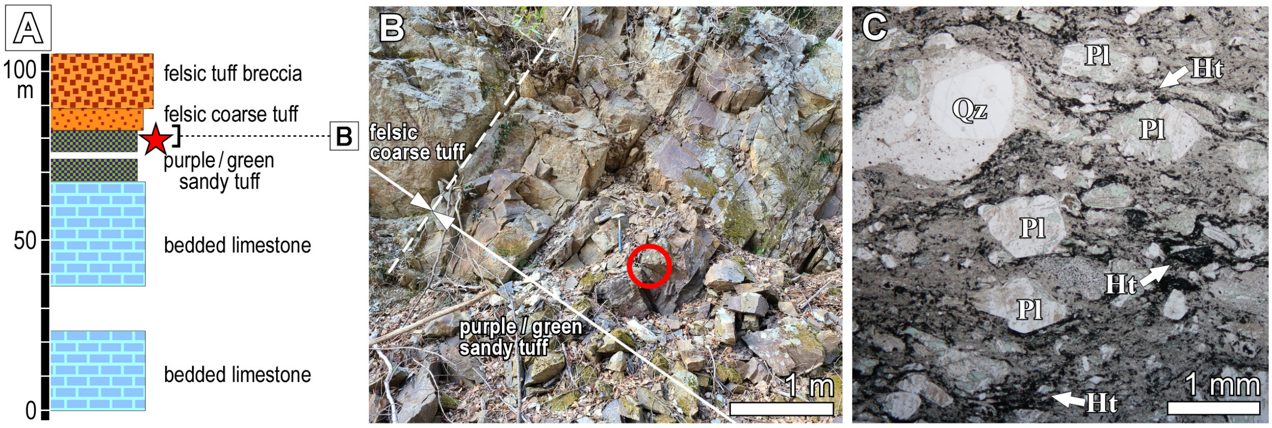

Fig. 4 (A) Columnar section around the horizon of the dating sample (22040115) in the upper Carboniferous Kidoguchi Formation. East of Shizu [39.05935N, 141.51294E], Oide area, Rikuzentakata City. The sampling horizon is shown as a red star. lp.: lapilli, br.: breccia. (B) Photo-image of the outcrop of the sample for dating. The sample was collected from the purple sandy tuff bed shown as red circle. Forest road cliff at east of Shizu, Oide area, Rikuzentakata City. Dashed line shows the boundary between the felsic coarse tuff bed and purple sandy tuff bed. (C) Thin-section photo-image of the dating sample. Its lithology shows coarse tuff containing fragments of quartz-bearing felsic volcanic rocks and grains of partly saussuritized plagioclase. Matrix is fine tuff with black hematitic spots and seams.
Ht: hematite, Pl: plagioclase, Qz: quartz.

or seams in the matrix. Brown oxidized chlorite occurs in plagioclase grains and within the matrix. Rare fine zircon grains occur within the tuff matrix.

4. Analytical methods

The extraction of zircon grains from the samples and subsequent dating analyses were conducted by Kyoto Fission-Track, Japan. Zircon U–Pb dating was also conducted using a multiple collector–inductively coupled plasma–mass spectrometer at the University of Tokyo, Tokyo, Japan. Instrumentation and operating conditions for the analyses are given in Table 1. Plešovice zircon (^{238}U–^{206}Pb age of 337.13 ± 0.37 Ma; Sláma *et al.*, 2008) was utilized as a primary standard. In addition, zircons OD-3 (^{238}U–^{206}Pb age of 33.0 ± 0.1 Ma; Iwano *et al.*, 2013), Nancy 91500 (^{238}U–^{206}Pb age of 1062.4 ± 0.4 Ma; Wiedenbeck *et al.*, 1995), and GJ-1 (^{238}U–^{206}Pb age of 610.0 ± 0.9 Ma; Jackson *et al.*, 2004) were used as secondary standards for quality control. Prior to analyses, a single laser shot was used to reduce lead contamination on zircon surfaces. During analyses, the laser was directed onto the center of each polished zircon surface, avoiding cracks and inclusions to ensure accurate data.

The ^{238}U–^{206}Pb age, which typically shows a smaller error than the ^{235}U–^{207}Pb age, was adopted for age determinations in this study. Assuming that the ^{206}Pb–^{238}U age is A ± B (A: age; B: 2σ error of the age) and the ^{207}Pb–^{235}U age is C ± D (C: age; D: 2σ error of the age), we considered analytical concordance if inequality 1 holds when the ^{207}Pb–^{235}U age is older than the ^{206}Pb–^{238}U age or if inequality 2 holds when the ^{207}Pb–^{235}U age is younger than the ^{207}Pb–^{235}U age:

$$\frac{(A+B)-(C-D)}{A} \times 100 > 0 \qquad (1)$$

$$\frac{(C+D)-(A-B)}{C} \times 100 \times (-1) < 0 \qquad (2)$$

Data processing was performed using Isoplot 4.15 software (Ludwig, 2012). Analytical results for the secondary standard (Tables 2 and 3) are within ±5% of recommended ages, suggesting that the results for the two samples (22040401-1 and 22040115) are reasonable.

5. Results

Isotopic data for sample 22040401-1 from the Shittakazawa Formation and sample 22040115 from the Kidoguchi Formation are summarized in Tables 2 and 3, respectively. We use the geological timescale of Gradstein *et al.* (2020) when considering the obtained U–Pb ages.

For sample 22040401-1, all 30 analyzed zircons yield concordant ages (Table 2; Fig. 5A). Most grains have ages of 350–330 Ma (early Carboniferous), with one Proterozoic grain (ca. 1360 Ma) that is interpreted as a xenocryst. The weighted mean age of the grains, except for the Proterozoic grain, is 339.5 ± 2.6 Ma (2σ error; n = 29; MSWD = 2.7, Fig. 5B).

For sample 22040115, 27 of the 30 zircons yield concordant ages (Table 3; Fig. 5C). The concordant grains have ages of 330–305 Ma (late Carboniferous). The weighted mean age of the concordant grains is 313.6 ± 2.3 Ma (2σ error; n = 27; MSWD = 1.6, Fig. 5D).

Table 1 Operating condition of the instrumentation of a multi-collector inductively coupled plasma mass spectrometry for the analysis.

Sample no.	22040401-1 (Shittakazawa Formation)	22040115 (Kidoguchi Formation)
Laser ablation		
Model	CARBIDE (Light Conversion)	same as on the left
Laser type	Femtosecond laser	
Pulse duration	290 fs	
Wave length	257 nm	
Energy density	3.8 J/cm	
Spot size	10 μm (single spot)	
Repetition rate	30 Hz	
Carrier gas (He)	0.60 L/min	
Duration of laser ablation	4 s	3.3 s
ICP–MS		
Model	Nu Plasma II (Nu Instruments)	ditto
ICP-MS type	Multi-collector	
Forward power	1300 W	
Make-up gas (Ar)	0.80 L/min	0.90 L/min
ThO^+/Th (oxide ratio)	<1%	ditto
Data acquisition protocol	Time-resolved analysis	
Data acquisition	9 s (6 s gas blank, 3 s ablation signal)	
Monitor isotopes	^{202}Hg, ^{204}Pb, ^{206}Pb, ^{207}Pb, ^{208}Pb, ^{232}Th, ^{235}U	
Standards		
Primary standard	Plešovice*1	
Secondary standard	OD-3*2, 3, 4 Nancy 91500*5 GJ-1*6	

*1: Sláma *et al.* (2008); *2: Iwano *et al.* (2012); *3: Iwano *et al.* (2013); *4: Lukács *et al.* (2015); *5: Wiedenbeck *et al.* (1995); *6: Jackson *et al.* (2004)

6. Discussions

Previous zircon U–Pb ages for Carboniferous clastic rocks in the SKB have been limited to data obtained from detrital grains in sandstones of the lower section. Okawa *et al.* (2013) presented a youngest concordant age of 348.9 ± 7.8 Ma (recalculated as the weighted mean age of a youngest cluster using the method of the present study: 350.3 ± 2.0 Ma [MSWD = 0.5]) for a sample from the western area (Karaumedate Formation, 1 in Fig. 2). Isozaki *et al.* (2014) presented a younger group of ages of 384–335 Ma (recalculated as above: 337.3 ± 4.0 Ma [MSWD = 1.5]) for a sample from the central area (Hikoroichi Formation, 8 in Fig. 2). In contrast to these previous data, our new zircon U–Pb ages from the sampled felsic tuffs should give more reliable depositional ages because most of the grains are syn-sedimentary. Accordingly, our new age data allow the duration of volcanism recorded in the Carboniferous strata of the SKB to be better constrained.

The age of 339.5 ± 2.6 Ma for the felsic tuff sample from the middle Shittakazawa Formation corresponds chronostratigraphically to the middle Visean (i.e., the Holkerian Substage in western Europe). This age is younger than the late Tournaisian age determined by the previous biostratigraphic correlation of the brachiopod fauna from the upper part of the formation (Tazawa and Kurita, 2019; Tazawa, 2020) or by lithostratigraphic comparison with the well-studied lower Hikoroichi Formation in the Hikoroichi area (Kawamura, 1985; Kawamura and Kawamura, 1989a). A similar early–middle Visean age has been assigned to the overlying Arisu Formation by correlation of the brachiopod fauna (Tazawa and Iryu, 2019; Tazawa, 2020). Therefore, the ages of the Shittakazawa and Arisu formations are likely to be slightly younger than previously estimated, although the ages of the basal to lower parts have yet to be clarified.

The age of 313.6 ± 2.3 Ma for the sandy tuff sample from the middle Kidoguchi Formation corresponds chronostratigraphically to the early Moscovian (i.e., Bolsovian Substage in western Europe). Previously, the age of the formation was tentatively assigned to the late Carboniferous based on the discovery of the fossil calcisponge *Chaetetes* (Ehiro and Mori, 1993), whose genera occur over a wide interval from the Ordovician

Table 2 U–Pb–Th isotopic data and U–Pb age of the zircon in the tuff in the Shittakazawa Formation determined using a multi-collector inductively coupled mass spectrometry.

Grain no.	Total count ^{206}Pb	^{207}Pb	^{208}Pb	^{232}Th	^{235}U	^{238}U	Th/U	Isotopic ratios $^{207}Pb/^{206}Pb$	Error 2σ	$^{206}Pb/^{238}U$	Error 2σ	$^{207}Pb/^{235}U$	Error 2σ	$^{208}Pb/^{232}Th$	Error 2σ	U–Pb age (Ma) $^{206}Pb/^{238}U$	Error 2σ	$^{207}Pb/^{235}U$	Error 2σ	Remark
1	32227	2086	3196	215313	5470	754184	0.46	0.0535	± 0.0030	0.0544	± 0.0017	0.4016	± 0.0238	0.0159	± 0.0008	341.4	± 11.1	342.8	± 23.8	
2	86526	9686	10648	168210	3399	468721	0.57	0.0926	± 0.0035	0.2350	± 0.0087	3.0010	± 0.1482	0.0676	± 0.0025	1360.5	± 55.8	1407.9	± 140.3	
3	74506	4862	14176	928650	12918	1781157	0.83	0.0540	± 0.0023	0.0532	± 0.0012	0.3964	± 0.0176	0.0163	± 0.0006	334.4	± 7.8	339.0	± 17.8	
4	81987	5275	11101	743451	14184	1955698	0.61	0.0532	± 0.0023	0.0534	± 0.0012	0.3917	± 0.0170	0.0159	± 0.0006	335.1	± 7.5	335.6	± 17.1	
5	51318	3433	5213	325348	8632	1190185	0.44	0.0553	± 0.0026	0.0549	± 0.0014	0.4189	± 0.0208	0.0171	± 0.0007	344.4	± 9.3	355.2	± 21.0	
6	39080	2539	5486	448263	6919	953944	0.75	0.0537	± 0.0028	0.0521	± 0.0015	0.3866	± 0.0212	0.0131	± 0.0005	327.7	± 9.7	331.9	± 21.3	
7	34776	2204	4044	262930	5949	820311	0.51	0.0524	± 0.0028	0.0540	± 0.0017	0.3902	± 0.0225	0.0164	± 0.0007	338.8	± 10.6	334.5	± 22.6	
8	166087	10685	33865	2186801	28129	3878389	0.90	0.0532	± 0.0020	0.0545	± 0.0010	0.4001	± 0.0148	0.0165	± 0.0006	342.1	± 6.2	341.7	± 14.9	
9	45938	2959	5629	366268	7613	1049657	0.56	0.0533	± 0.0026	0.0557	± 0.0015	0.4094	± 0.0214	0.0164	± 0.0007	349.5	± 9.9	348.4	± 21.5	
10	53140	3459	6858	479070	9202	1268804	0.60	0.0538	± 0.0025	0.0533	± 0.0014	0.3959	± 0.0196	0.0153	± 0.0006	334.8	± 8.8	338.7	± 19.7	
11	84583	5388	15553	976736	13835	1907578	0.82	0.0527	± 0.0022	0.0564	± 0.0012	0.4102	± 0.0178	0.0170	± 0.0006	353.9	± 8.0	349.0	± 17.9	
12	55236	3534	5978	393235	9370	1291967	0.49	0.0529	± 0.0025	0.0544	± 0.0014	0.3972	± 0.0195	0.0162	± 0.0007	341.6	± 8.9	339.6	± 19.6	
13	35611	2251	4506	303314	6240	860373	0.56	0.0523	± 0.0028	0.0527	± 0.0016	0.3799	± 0.0217	0.0159	± 0.0007	331.0	± 10.2	327.0	± 21.8	
14	29403	1909	2472	161290	4943	681508	0.38	0.0537	± 0.0031	0.0549	± 0.0018	0.4068	± 0.0249	0.0164	± 0.0008	344.6	± 11.7	346.6	± 25.0	
15	47283	3118	4292	266703	8297	1144054	0.37	0.0545	± 0.0027	0.0526	± 0.0014	0.3958	± 0.0202	0.0172	± 0.0008	330.5	± 9.1	338.6	± 20.3	
16	40323	2722	4133	255809	6937	956495	0.42	0.0556	± 0.0027	0.0534	± 0.0015	0.4096	± 0.0212	0.0172	± 0.0009	335.5	± 10.0	348.6	± 21.3	
17	80505	5517	14226	920234	13454	1855016	0.79	0.0564	± 0.0023	0.0550	± 0.0012	0.4281	± 0.0174	0.0165	± 0.0007	345.1	± 8.0	361.8	± 17.5	
18	68772	4477	6462	395713	11227	1548014	0.41	0.0536	± 0.0023	0.0563	± 0.0014	0.4163	± 0.0180	0.0174	± 0.0008	353.0	± 8.7	353.4	± 18.2	
19	24076	1603	4017	262305	4029	555463	0.75	0.0548	± 0.0033	0.0549	± 0.0020	0.4153	± 0.0267	0.0163	± 0.0009	344.7	± 12.9	352.7	± 26.7	
20	83514	5692	13790	913269	14195	1957147	0.74	0.0561	± 0.0022	0.0541	± 0.0012	0.4187	± 0.0168	0.0161	± 0.0007	339.5	± 7.7	355.1	± 16.9	
21	218593	14421	37140	2399748	37369	5152418	0.74	0.0543	± 0.0018	0.0538	± 0.0009	0.4029	± 0.0128	0.0165	± 0.0007	337.6	± 5.9	343.7	± 12.9	
22	141672	9255	27023	1738180	24203	3337085	0.83	0.0538	± 0.0020	0.0538	± 0.0010	0.3992	± 0.0140	0.0166	± 0.0007	337.8	± 6.6	341.1	± 14.1	
23	56306	3677	5499	368790	9649	1330375	0.44	0.0538	± 0.0024	0.0536	± 0.0014	0.3979	± 0.0184	0.0159	± 0.0008	336.8	± 8.8	340.1	± 18.5	
24	62096	3875	9518	626363	10259	1414504	0.70	0.0514	± 0.0023	0.0556	± 0.0014	0.3943	± 0.0179	0.0162	± 0.0008	349.0	± 8.9	337.5	± 18.0	
25	42736	2775	3192	205223	7201	992834	0.33	0.0535	± 0.0026	0.0545	± 0.0016	0.4023	± 0.0206	0.0166	± 0.0009	342.4	± 10.0	343.3	± 20.7	
26	82077	5438	7081	465319	14044	1936389	0.38	0.0545	± 0.0022	0.0537	± 0.0012	0.4042	± 0.0164	0.0162	± 0.0008	337.3	± 7.7	344.7	± 16.5	
27	45380	2847	5344	334769	7518	1036621	0.51	0.0517	± 0.0025	0.0555	± 0.0016	0.3954	± 0.0200	0.0170	± 0.0009	348.0	± 10.0	338.3	± 20.1	
28	90449	5946	12560	796381	15366	2118656	0.60	0.0541	± 0.0021	0.0541	± 0.0012	0.4040	± 0.0160	0.0168	± 0.0008	339.6	± 7.6	344.5	± 16.1	
29	392965	25952	62981	4250842	68821	9489075	0.71	0.0544	± 0.0017	0.0525	± 0.0008	0.3937	± 0.0114	0.0158	± 0.0007	329.7	± 5.2	337.1	± 11.5	
30	74073	4884	7535	482486	12449	1716404	0.45	0.0543	± 0.0023	0.0547	± 0.0013	0.4096	± 0.0172	0.0167	± 0.0008	343.2	± 8.2	348.6	± 17.3	
Secondary standards																				
GJ1 1-1	103368	7648	1346	56301	9659	1331755	0.07	0.0612	± 0.0021	0.0994	± 0.0027	0.8391	± 0.0316	0.0257	± 0.0017	610.7	± 17.1	618.6	± 31.5	
GJ1 1-2	101654	7664	1455	51099	9781	1348651	0.06	0.0624	± 0.0021	0.0965	± 0.0026	0.8303	± 0.0312	0.0306	± 0.0020	593.9	± 16.5	613.8	± 31.1	
GJ1 1-3	106436	7846	1428	38821	10224	1409745	0.04	0.0610	± 0.0021	0.0967	± 0.0025	0.8131	± 0.0302	0.0395	± 0.0026	594.8	± 16.3	604.2	± 30.2	
GJ1 1-4	101251	7452	1422	57796	9593	1322722	0.07	0.0609	± 0.0021	0.0980	± 0.0026	0.8232	± 0.0311	0.0264	± 0.0018	602.7	± 16.9	609.8	± 31.1	
GJ1 1-5	96498	6826	1273	50206	9237	1273625	0.06	0.0585	± 0.0021	0.0970	± 0.0026	0.7831	± 0.0303	0.0272	± 0.0019	596.8	± 16.9	587.2	± 30.3	
OD3 1-1	8603	491	2639	1783810	15563	2145827	1.30	0.0472	± 0.0045	0.0051	± 0.0002	0.0334	± 0.0031	0.0016	± 0.0001	33.0	± 1.0	33.4	± 3.2	
OD3 1-2	4298	272	1121	763275	8047	1109508	1.08	0.0522	± 0.0067	0.0050	± 0.0002	0.0358	± 0.0045	0.0016	± 0.0001	31.9	± 1.3	35.7	± 4.5	
OD3 1-3	5727	269	1568	1048708	10342	1426019	1.15	0.0389	± 0.0049	0.0051	± 0.0002	0.0276	± 0.0035	0.0016	± 0.0001	33.1	± 1.2	27.6	± 3.5	*discordant*
OD3 1-4	12112	720	4023	2723533	22155	3054666	1.40	0.0491	± 0.0040	0.0051	± 0.0001	0.0344	± 0.0027	0.0016	± 0.0001	32.6	± 0.9	34.4	± 2.8	
OD3 1-5	11190	697	3732	2475113	20329	2802929	1.39	0.0515	± 0.0042	0.0051	± 0.0001	0.0363	± 0.0029	0.0016	± 0.0001	32.9	± 0.9	36.2	± 2.9	
91500 4-1	62880	5717	5566	115191	3345	461206	0.36	0.0737	± 0.0039	0.1753	± 0.0068	1.7821	± 0.1132	0.0539	± 0.0075	1041.2	± 43.4	1038.9	± 108.9	
91500 4-2	63952	5550	5652	112155	3345	461275	0.35	0.0703	± 0.0037	0.1782	± 0.0069	1.7298	± 0.1102	0.0562	± 0.0078	1057.4	± 44.1	1019.7	± 106.1	

Table 3 U–Pb–Th isotopic data and U–Pb age of the zircon in the tuff in the Kidoguchi Formation determined using a multi-collector inductively coupled mass spectrometry.

Grain no.	Total count							Isotopic ratios								U–Pb age (Ma)				Remark
	^{206}Pb	^{207}Pb	^{208}Pb	^{232}Th	^{235}U	^{238}U	Th/U	$^{207}Pb/^{206}Pb$	Error 2σ	$^{206}Pb/^{238}U$	Error 2σ	$^{207}Pb/^{235}U$	Error 2σ	$^{208}Pb/^{232}Th$	Error 2σ	$^{206}Pb/^{238}U$	Error 2σ	$^{207}Pb/^{235}U$	Error 2σ	
1	255860	16896	53410	1646050	43741	6030956	0.86	0.0530	± 0.0016	0.0498	± 0.0010	0.3636	± 0.0107	0.0147	± 0.0009	313.0	± 6.7	314.9	± 10.8	
2	434006	30220	121590	4310937	80819	11143279	1.22	0.0558	± 0.0016	0.0457	± 0.0009	0.3519	± 0.0094	0.0127	± 0.0007	287.9	± 5.8	306.2	± 9.5	*discordant*
3	56638	3585	10633	300412	9741	1343133	0.71	0.0508	± 0.0022	0.0495	± 0.0014	0.3464	± 0.0157	0.0160	± 0.0010	311.2	± 9.1	302.0	± 15.9	
4	22450	1544	1820	52216	3725	513539	0.32	0.0552	± 0.0032	0.0513	± 0.0020	0.3902	± 0.0253	0.0157	± 0.0012	322.3	± 13.1	334.5	± 25.4	
5	44117	2974	7416	217881	7623	1051033	0.66	0.0541	± 0.0025	0.0492	± 0.0015	0.3673	± 0.0180	0.0154	± 0.0010	309.8	± 9.8	317.6	± 18.1	
6	34138	2255	3439	97689	5651	779145	0.40	0.0530	± 0.0027	0.0514	± 0.0017	0.3756	± 0.0206	0.0159	± 0.0011	323.0	± 11.3	323.8	± 20.7	
7	30037	4834	10674	206364	4974	685846	0.95	0.1291	± 0.0052	0.0514	± 0.0018	0.9146	± 0.0426	0.0234	± 0.0014	322.9	± 11.8	659.5	± 42.4	*discordant*
8	37254	2604	4838	139368	6284	866441	0.51	0.0561	± 0.0027	0.0504	± 0.0017	0.3901	± 0.0203	0.0157	± 0.0010	317.1	± 10.7	334.4	± 20.4	
9	71814	4759	12345	347047	12049	1661306	0.66	0.0531	± 0.0021	0.0507	± 0.0014	0.3717	± 0.0154	0.0161	± 0.0010	318.8	± 8.8	320.9	± 15.5	
10	45970	3121	5988	168434	8086	1114955	0.48	0.0544	± 0.0024	0.0484	± 0.0015	0.3633	± 0.0175	0.0161	± 0.0010	304.4	± 9.4	314.6	± 17.6	
11	33275	2252	3375	93470	5754	793384	0.37	0.0543	± 0.0027	0.0492	± 0.0017	0.3683	± 0.0202	0.0163	± 0.0011	309.5	± 10.7	318.4	± 20.3	
12	62018	4063	9158	258644	10533	1452291	0.56	0.0525	± 0.0022	0.0501	± 0.0014	0.3631	± 0.0158	0.0160	± 0.0010	315.0	± 9.0	314.5	± 15.9	
13	33110	2217	4798	140015	5728	789833	0.56	0.0537	± 0.0027	0.0492	± 0.0017	0.3642	± 0.0201	0.0155	± 0.0010	309.4	± 10.7	315.4	± 20.2	
14	572723	37506	130549	3762396	96592	13318128	0.89	0.0525	± 0.0014	0.0504	± 0.0010	0.3655	± 0.0096	0.0157	± 0.0009	317.2	± 6.3	316.3	± 9.7	
15	33642	2182	4955	150240	5566	767493	0.62	0.0520	± 0.0026	0.0514	± 0.0018	0.3690	± 0.0205	0.0149	± 0.0010	323.2	± 11.3	318.9	± 20.6	
16	49516	3317	8056	230650	8374	1154604	0.63	0.0537	± 0.0024	0.0503	± 0.0015	0.3729	± 0.0176	0.0158	± 0.0010	316.3	± 9.7	321.8	± 17.7	
17	42056	2899	4567	141332	7029	969114	0.46	0.0553	± 0.0025	0.0509	± 0.0016	0.3882	± 0.0194	0.0146	± 0.0010	320.0	± 10.3	333.0	± 19.5	
18	49718	3508	7110	209755	8816	1215492	0.55	0.0565	± 0.0025	0.0481	± 0.0014	0.3753	± 0.0176	0.0153	± 0.0009	302.9	± 9.3	323.6	± 17.7	
19	70344	4642	11931	366000	12310	1697308	0.69	0.0529	± 0.0021	0.0487	± 0.0013	0.3556	± 0.0151	0.0147	± 0.0008	306.8	± 8.6	308.9	± 15.2	
20	73006	4889	10040	289942	12600	1737231	0.53	0.0537	± 0.0021	0.0494	± 0.0013	0.3659	± 0.0153	0.0156	± 0.0008	311.0	± 8.7	316.6	± 15.4	
21	98706	6753	23598	668555	16887	2328441	0.92	0.0548	± 0.0020	0.0499	± 0.0013	0.3771	± 0.0143	0.0159	± 0.0008	313.6	± 8.2	324.9	± 14.4	
22	63501	4597	7618	207813	10682	1472773	0.45	0.0580	± 0.0023	0.0507	± 0.0014	0.4058	± 0.0175	0.0165	± 0.0009	318.9	± 9.3	345.8	± 17.6	*discordant*
23	65544	4335	8657	241901	11065	1525663	0.51	0.0530	± 0.0021	0.0505	± 0.0014	0.3694	± 0.0161	0.0161	± 0.0009	317.7	± 9.2	319.2	± 16.2	
24	80644	5458	14983	438083	14120	1946870	0.72	0.0542	± 0.0021	0.0487	± 0.0013	0.3645	± 0.0147	0.0154	± 0.0008	306.6	± 8.3	315.6	± 14.8	
25	48126	3223	7548	224422	8121	1119715	0.64	0.0537	± 0.0024	0.0505	± 0.0016	0.3743	± 0.0181	0.0151	± 0.0008	317.9	± 10.0	322.8	± 18.2	
26	31041	2065	4401	119790	5044	695436	0.55	0.0533	± 0.0028	0.0525	± 0.0019	0.3861	± 0.0223	0.0165	± 0.0010	329.8	± 12.1	331.5	± 22.4	
27	52671	3524	7474	218751	8888	1225424	0.57	0.0536	± 0.0023	0.0505	± 0.0015	0.3739	± 0.0175	0.0154	± 0.0009	317.9	± 9.7	322.6	± 17.6	
28	80092	5339	13343	390779	13918	1919010	0.65	0.0534	± 0.0020	0.0491	± 0.0013	0.3617	± 0.0147	0.0154	± 0.0008	308.9	± 8.4	313.5	± 14.8	
29	48773	3169	6710	208326	8456	1165914	0.57	0.0521	± 0.0023	0.0492	± 0.0015	0.3534	± 0.0171	0.0145	± 0.0008	309.6	± 9.6	307.3	± 17.2	
30	37727	2501	5719	169237	6495	895471	0.60	0.0531	± 0.0026	0.0495	± 0.0016	0.3632	± 0.0193	0.0152	± 0.0009	311.7	± 10.5	314.6	± 19.4	
Secondary standards																				
91500 7-1	145109	13713	13500	122536	6867	946773	0.41	0.0757	± 0.0024	0.1802	± 0.0056	1.8831	± 0.0725	0.0496	± 0.0026	1068.3	± 36.2	1075.2	± 71.1	
91500 7-2	132308	12399	12543	119455	6358	876577	0.44	0.0751	± 0.0024	0.1775	± 0.0057	1.8390	± 0.0726	0.0472	± 0.0025	1053.3	± 36.6	1059.5	± 71.2	
GJ1 7-1	230646	17235	3378	50921	20745	2860305	0.06	0.0599	± 0.0018	0.0948	± 0.0023	0.7834	± 0.0252	0.0299	± 0.0018	584.0	± 14.7	587.4	± 25.3	
GJ1 7-2	237174	18034	3483	65900	21174	2919482	0.07	0.0609	± 0.0018	0.0955	± 0.0023	0.8031	± 0.0256	0.0238	± 0.0015	588.2	± 14.7	598.6	± 25.7	
OD3 7-1	21134	1192	6663	1910007	36186	4989374	1.22	0.0452	± 0.0029	0.0050	± 0.0001	0.0311	± 0.0020	0.0016	± 0.0001	32.0	± 0.8	31.1	± 2.0	
OD3 7-2	33413	2033	10703	3061315	56760	7826096	1.25	0.0488	± 0.0026	0.0050	± 0.0001	0.0338	± 0.0017	0.0016	± 0.0001	32.3	± 0.8	33.7	± 1.8	

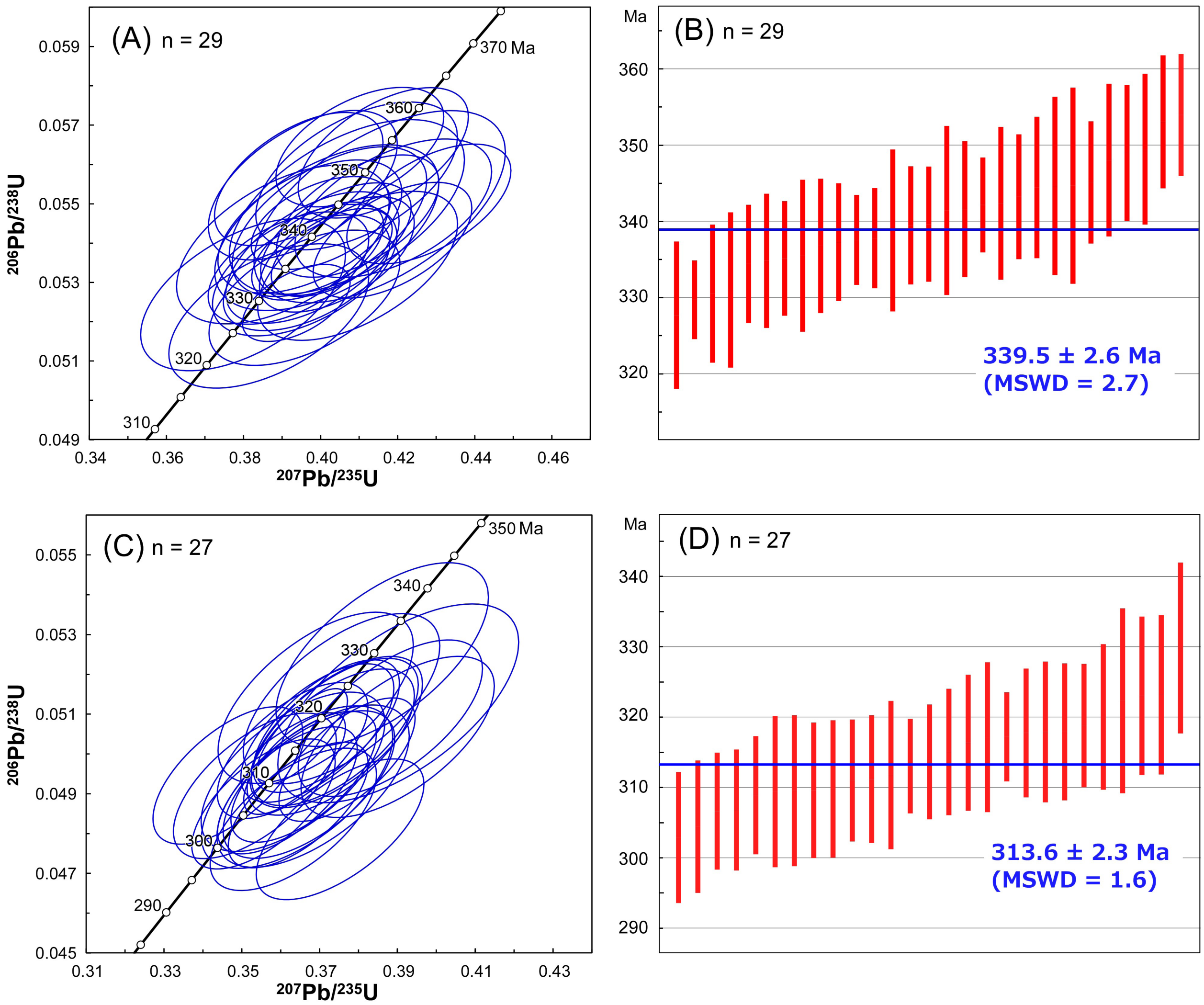

Fig. 5 Results of U–Pb dating for the concordant zircons from the coarse tuff in the Shittakazawa Formation and the sandy tuff in the Kidoguchi Formation. (A) Concordia diagram of the former except for a Proterozoic zircon grain. (B) Weighted mean age of the former. (C) Concordia diagram of the latter. (D) Weighted mean age of the latter.
Error is 2σ. MSWD: mean squared weighted deviation, n: number.

to Jurassic but are most common in the middle–upper Carboniferous in Japan (Minato, 1975). Hence, the age determined in this study more tightly constrains the age of the Kidoguchi Formation in the SKB compared with previous age estimations.

The two new zircon U–Pb ages and the lithologies of the abundant volcanic rocks among the lower Carboniferous suggest continuous volcanism in the SKB from the Visean to Moscovian. The Visean volcanism, which may have begun during the late Tournaisian, is considered to have occurred in a back-arc to intra-arc setting under crustal extension, along with the formation of heterogeneous sedimentary basins (Kawamura and Kawamura, 1989b). The subsequent Serpukhovian to Moscovian volcanism appears to have been less active than that of the earlier period, resulting in the dominance of shallow-marine carbonates influenced by sea-level fluctuations. However, it remains unclear whether the Visean bimodal volcanism continued into the late Carboniferous, as geochemical signatures for the late Carboniferous volcanic rocks have not been investigated in detail.

Tsuchiya *et al.* (2014) reported zircon U–Pb ages of 308–302 Ma for the Wariyama sheared granodiorite (Fujita *et al.*, 1988) at the eastern margin of the Abukuma Massif (Fig. 1A). Li and Takeuchi (2021) presented weighted mean ages of 311–266 Ma for the youngest clusters of zircons from five granitic clasts of Usuginu-type conglomerate. These ages are slightly younger than the age of tuff from the Kidoguchi Formation, possibly implying volcanism and plutonism within or near the SKB during the late Carboniferous. In addition, minor andesitic tuff occurs in the lowermost

Permian deposits, which overlie Carboniferous strata across a regional unconformity (Kawamura *et al.*, 1990; Yoshida *et al.*, 1994). The above synthesis of evidence indicates essentially continuous magmatism from the late Carboniferous to the early Permian, although less intense than the early Carboniferous volcanism.

7. Conclusion

Carboniferous strata in the SKB contain large volumes of volcanic rocks in the lower section and moderate volumes of volcaniclastic rocks in the upper section. According to previous studies, the former rocks were produced by bimodal volcanism in and around back-arc to intra-arc regions, whereas the latter rocks resulted from intermittent eruptions.

Zircon U–Pb dating was conducted on two tuff samples from Carboniferous felsic volcaniclastic rocks in the SKB. These samples, from the early Carboniferous Shittakazawa Formation and the late Carboniferous Kidoguchi Formation, yielded weighted mean ages of 339.5 ± 2.6 Ma (middle Visean) and 313.6 ± 2.3 Ma (early Moscovian), respectively. These ages are slightly younger than the depositional ages of the formations, as determined from paleontological data in previous studies. These precise ages provide tighter constraints on the duration of Carboniferous volcanism in the SKB. The change from Carboniferous intense volcanism (including concurrent plutonism) to early Permian minor volcanism represents a key geotectonic transition in the long geological history of the SKB.

Acknowledgements: The author thanks Drs. Danhara T. and Iwano H. (Kyoto Fission-Track Co., Ltd.) for LA–ICP–MS analyses; We are grateful to Dr. Suzuki K. for careful reviews of the manuscript. Field works in this study were partly supported by JSPS KAKENHI (Grant Number 21K02566).

References

Ehiro, M. and Mori, K. (1993) Discovery of *Chaetetes* from the Kidoguchi Formation of the western part of Yahagi-machi, Rikuzen-takata City, Southern Kitakami Mountains and its significance. *Journal of the Geological Society of Japan*, **99**, 407–410 (in Japanese).

Ehiro, M., Tsujimori, T., Tsukada, K. and Nuramkhaan, M. (2016) Paleozoic basement and associated cover. In Moreno, T., Wallis, S., Kojima, T. and Gibbons, W., eds., *The Geology of Japan*, Geological Society of London, 25–60.

Fujita, Y., Kano, H., Takizawa, F. and Yashima, R. (1988) *Geology of the Kakuda district*. With geological sheet map at 1:50,000, Geological Survey of Japan, 99p. (in Japanese with English abstract).

Geological Survey of Japan, AIST (2022) Seamless digital geological map of Japan V2 1:200,000. https://gbank.gsj.jp/seamless [Accessed: 2023-09-01].

Gradstein, F. M., Ogg, J. G., Schmitz, M. D. and Ogg, G. M. (2020) *The Geologic Time Scale 2020*. Elsevier, Amsterdam, 1357p. doi:10.1016/C2020-1-02369-3

Isozaki. Y., Aoki, K., Sakata, S. and Hirata, T. (2014) The eastern extension of Paleozoic South China in NE Japan evidenced by detrital zircon. *GFF*, **136**, 116–119.

Iwano, H., Orihashi, Y., Danhara, T., Hirata, T. and Ogasawara, M. (2012) Evaluation of fission-track and U–Pb double dating method for identical zircon grains: Using homogeneous zircon grains in Kawamoto Granodiorite in Shimane prefecture, Japan. *Journal of the Geological Society of Japan*, **118**, 365–375.

Iwano, H., Orihashi, Y., Hirata, T., Ogasawara, M., Danhara, T., Horie, K., Hasebe, N., Sueoka, S., Tamura, A., Hayasaka, Y., Katsube, A., Ito, H., Tani, K., Kimura, J., Chang, Q., Kouchi, Y., Haruta, Y. and Yamamoto, K. (2013) An inter-laboratory evaluation of OD-3 zircon for use as a secondary U–Pb dating standard. *Island Arc*, **22**, 382–394.

Jackson, S. E, Pearson, N. J., Griffin, W. L. and Belousova, E. A. (2004) The application of laser ablation-inductively coupled plasma-mass spectrometry to in situ U–Pb zircon geochronology. *Chemical Geology*, **211**, 47–69.

Kawamura, M. (1997) Occurrence and chemical composition of the Early Carboniferous island arc-type volcanic rocks of the Setamai District, South Kitakami Terrane, N. E. Japan. *Commemorative Volume for Professor Makoto Kato*, 77–92 (in Japanese with English abstract).

Kawamura, M. (1985) Lithostratigraphy of the Carboniferous Formations in the Setamai region, Southern Kitakami Belt, Northeast Japan (part 1) – Shimoarisu district of the Setamai Subbelt–. *Journal of the Geological Society of Japan*, **91**, 165–178 (in Japanese with English abstract).

Kawamura, M., Kato, M. and Kitakami Paleozoic Research Group (1990) Southern Kitakami Terrane. *In* Ichikawa, K., Mizutani, S., Hara, I. and Yao, A., eds., *Pre-Cretaceous Terranes of Japan*. Publication of IGCP Project No. 224: Pre-Jurassic Evolution of Eastern Asia. Osaka, 249–266.

Kawamura, T. (1983) The Lower Carboniferous formations in the Hikoroichi region, southern Kitakami Mountain, northeast Japan (Part 1) – Stratigraphy of the Hikoroichi Formation –. *Journal of the Geological Society of Japan*, **89**, 707–722 (in Japanese with English abstract).

Kawamura, T. and Kawamura, M. (1989a) The Carboniferous System of the South Kitakami Terrane, northeast Japan (Part 1) – Summary of the stratigraphy –. *Earth Science (Chikyu Kagaku)*, **43**, 84–97 (in Japanese with English abstract).

Kawamura, T. and Kawamura, M. (1989b) The Carboniferous System of the South Kitakami Terrane, northeast Japan (Part 2) – Sedimentary and tectonic environment –. *Earth Science (Chikyu Kagaku)*, **43**, 157–167 (in Japanese with English abstract).

Kobayashi, F. (1973) On the Middle Carboniferous Nagaiwa Formation. *Journal of the Geological Society of Japan*, **79**, 69–78 (in Japanese with English abstract).

Li, Y. and Takeuchi, M. (2021) U–Pb dating of detrital zircon from Permian successions of the South Kitakami Belt, Northeast Japan: Clues to the paleogeography of the belt. *Island Arc*, **31**, e12435. doi: 10.1111/iar.12435

Ludwig, K. R. (2012). Isoplot 3.75: Geochronological Toolkit for Microsoft Excel. *Berkeley Geochronology Center Special Publication*, **5**, 75p.

Lukács, R., Harangi, S., Bachmann, O., Guillong, M., Danišík, M., Buret, Y., von Quadt, A., Dunkl, I., Fodor, L., Sliwinski J., Soós, I. and Szepesi, J. (2015) Zircon geochronology and geochemistry to constrain the youngest eruption events and magma evolution of the Mid-Miocene ignimbrite flare-up in the Pannonian Basin, eastern central Europe. *Contributions to Mineralogy and Petrology*, **170**, 1–26.

Minato, M. (1975) Japanese Palaeozoic corals. *Journal of the Geological Society of Japan*, **81**, 103–126.

Minato, M., Hunahashi, M., Watanabe, J. and Kato, M., eds. (1979) V*ariscan geohistory of northern Japan: The Abean Orogeny*, Tokai University Press, Tokyo, 427p.

Niikawa, I. (1983) Biostratigraphy and correlation of the Onimaru Formation in the southern Kitakami Mountains, Part II Correlation and conclusion. *Journal of the Geological Society of Japan*, **89**, 549–557 (in Japanese with English abstract).

Okawa, H., Shimojo, M., Orihashi, Y., Yamamoto, K., Hirata, T., Sano, S., lshizaki, Y., Kouchi, Y., Yanai, S. and Otoh, S. (2013) Detrital zircon geochronology of the Silurian–Lower Cretaceous continuous succession of the South Kitakami Belt, northeast Japan. *Memoir of the Fukui Prefectural Dinosaur Museum*, **12**, 35–78.

Pastor-Galán, D., Spencer, C. J., Furukawa, T. and Tsujimori T. (2021) Evidence for crustal removal, tectonic erosion and flare-ups from the Japanese evolving forearc sediment provenance. *Earth and Planetary Science Letters*, **564**, 116893. doi:10.1016/j.epsl.2021.116893

Sláma, J., Košler, J., Condon, J. D., Crowley, J. L., Gerdes, A., Hanchar, J. M., Horstwood, M. S. A., Morris, G. A., Nasdata, L., Norberg, N., Shaltegger, U., Schoene, B., Tubrett, M. N. and Whitehouse, M. J. (2008) Plešovice zircon – A new natural reference material for U–Pb and Hf isotopic microanalysis. *Chemical Geology*, **249**, 1–35.

Tazawa, J. (2020) Early Carboniferous (Mississippian) brachiopods from the Shittakazawa, Arisu and Odaira formations, South Kitakami Belt, Japan. *Memoir of the Fukui Prefectural Dinosaur Museum*, **19**, 11–88.

Tazawa, J. and Iryu, Y. (2019) Early Carboniferous (early Visean) brachiopod fauna from the middle part of the Arisu Formation in the Shimoarisu area, South Kitakami Belt, Japan. *Paleontological Research*, **23**, 95–109.

Tazawa, J., and Kurita, H. (2019) Early Carboniferous (late Tournaisian) brachiopod fauna from the Shittakazawa Formation in the Okuhinotsuchi area, South Kitakami Belt, Japan. *Journal of the Geological Society of Japan*, **125**, 219–225 (in Japanese).

Tsuchiya, N., Takeda, T., Tani, K., Adachi, T., Nakano, N., Osanai, Y. and Kimura, J. (2014) Zircon U–Pb age and its geological significance of late Carboniferous and Early Cretaceous adakitic granites from eastern margin of the Abukuma Mountains, Japan. *Journal of the Geological Society of Japan*, **120**, 37–51.

Yang, W. P. and Tazawa, J. (2000) Early Carboniferous miospores from the southern Kitakami Mountains, northeast Japan. *Paleontological Research*, **4**, 57–67.

Yoshida, K., Kawamura, M. and Machiyama, H. (1994) Transition in the composition of the Permian clastic rocks in the South Kitakami Terrane, Northeast Japan. *Journal of the Geological Society of Japan*, **100**, 744–761 (in Japanese with English abstract).

Wiedenbeck, M., Alle, P., Corfu, F., Griffin, W. L., Meier, M., Oberli, F., von Quadt, A., Roddick, J. C. and Spiegel, W. (1995) Three natural zircon standards for U–Th–Pb, Lu–Hf, trace element and REE analyses. *Geostandards Newsletter*, **19**, 1–23.

Recieved November 24, 2023
Accepted April 15, 2024
Published on-line May 16, 2024

ジルコン U–Pb 年代測定による南部北上帯の石炭紀火山活動期の制約

川村　寿郎・内野　隆之

要　旨

南部北上帯の石炭系は多量の火山砕屑岩を含み，特にそれが多い下部では当時の激しい火山活動を物語っている．今回，石炭系の下部及び上部に挟在する珪長質凝灰岩について，ジルコン U–Pb 年代測定を行った．下部に関しては尻高沢（しったかざわ）層中部の粗粒凝灰岩を，上部に関しては木戸口（きどぐち）層中部の紫色砂質凝灰岩を対象とした．測定の結果，前者からは 339.5 ± 2.6 Ma（ビゼーアン期中期），後者からは 313.6 ± 2.3 Ma（モスコビアン期前期）の年代が得られた．前者の年代は，尻高沢層が，これまでの化石産出と岩相層序対比で想定された年代（トルネーシアン期後期）よりも若くなることを示す．一方，後者の年代は，当該火山活動が石炭紀後期まで継続したことを確実にする．南部北上帯内における少量の石炭紀後期花崗岩類や最下部ペルム系の安山岩質凝灰岩の存在を考慮に入れると，同帯の火成活動は石炭紀前期で最も激しく，やや沈静化していくもののペルム紀前期まで長期にわたって継続したことが示唆される．

難読･重要地名

Arisu：有住，Hikoroichi：日頃市，Karaumedate：唐梅館，Kashiwari：柏里，Kidoguchi：木戸口，Komata：小股，Oide：生出，Omata：大股，Setamai：世田米，Shittakazawa：尻高沢，Shizu：清水，Tassobe：達曽部，Usuginu：薄衣，Wariyama：割山，Yahagi：矢作